

Piezotronic Effect Modulated Flexible AlGaIn/GaN High-Electron-Mobility Transistors

Jiyuan Zhu,^{†,‡,§} Xingyu Zhou,^{†,‡,§} Liang Jing,^{†,‡} Qilin Hua,^{†,‡,§} Weiguo Hu,^{*,†,‡,§} and Zhong Lin Wang^{*,†,‡,§,||}

[†]CAS Center for Excellence in Nanoscience, Beijing Key Laboratory of Micro-Nano Energy and Sensor, Beijing Institute of Nanoenergy and Nanosystems, Chinese Academy of Sciences, Beijing 100083, China

[‡]School of Nanoscience and Technology, University of Chinese Academy of Sciences, Beijing 100049, China

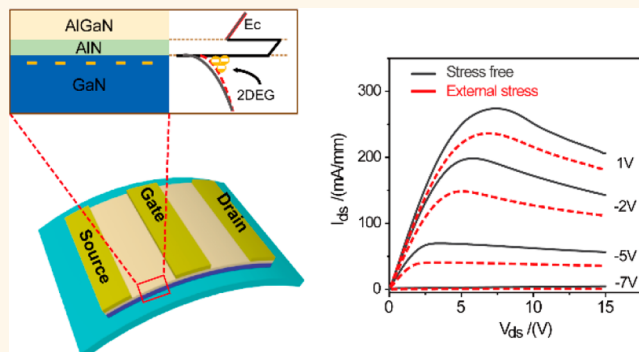
[§]Center on Nanoenergy Research, School of Physical Science and Technology, Guangxi University, Nanning 530004, China

^{||}School of Materials Science and Engineering, Georgia Institute of Technology, Atlanta, Georgia 30332-0245, United States

Supporting Information

ABSTRACT: Flexible electronic technology has attracted great attention due to its wide range of potential applications in the fields of healthcare, robotics, and artificial intelligence, *etc.* In this work, we have successfully fabricated flexible AlGaIn/GaN high-electron-mobility transistors (HEMTs) arrays through a low-damage and wafer-scale substrate transfer technology from a rigid Si substrate. The flexible AlGaIn/GaN HEMTs have excellent electrical performances with the $I_{d,max}$ achieving 290 mA/mm at $V_{gs} = +2$ V and the $g_{m,max}$ reaching to 40 mS/mm. The piezotronic effect provides a different freedom to optimize device performances, and flexible HEMTs can endure the larger mechanical distortions. Based on the piezotronic effect, we applied an external stress to significantly modulate the electrical performances of flexible HEMTs. The piezotronic effect modulated flexible AlGaIn/GaN HEMTs exhibit great potential in human-machine interface, intelligent microinductor systems, and active sensors, *etc.*, and introduce an opportunity to sensing or feedback external mechanical stimuli and so on.

KEYWORDS: AlGaIn/GaN high-electron-mobility transistors, flexible substrate, piezotronic effect, two-dimensional electron gas, wafer-scale



In recent years, flexible electronic technology has shown a rapid development trend,¹ opening a wide range of potential applications for energy harvesting, medical healthcare, consumer electronics, robotics, *etc.*² Thanks to the high saturation drift velocity, high sheet carrier concentration, wide band gap, and excellent frequency characteristics,³ AlGaIn/GaN high-electron-mobility transistors (HEMTs) are the best candidates for radio frequency (RF), microwave devices and power devices and so on.⁴ The flexible HEMTs are expected to satisfy the urgent requirements of the wireless communication and electrical supply in flexible electronics. However, due to the limitation of growth kinetics, AlGaIn/GaN HEMTs are usually fabricated on rigid substrates such as Si, sapphire, or SiC, thus they cannot be applied to nonplanar environments and are hard to deform. The substrate transfer technology has received a lot of attention and rapid developments, and some flexible AlGaIn/GaN HEMTs have been fabricated with various substrate transfer technologies, for example, a mechanical lapping and etching,⁵ a sacrificial 2D

boron nitride layer,⁶ and a xenon difluoride etching.⁷ Alleviating the devices performances degradation on flexible substrates is still a significant issue. In addition, flexible substrates provide some different functions such as flexible structures, stretchable structures, and curved conformal installations, which induce complex stress distribution to greatly affect the electrical characteristics.⁸

The piezotronic effect proposed by Z. L. Wang utilizes piezoelectric polarization charge to change the energy band structure at the interface or junction to control carrier transport.^{9–12} III-nitrides are ideal piezotronic materials and have wide industrial applications. The AlGaIn and GaN have strong spontaneous polarization and piezoelectric polarization, resulting in a strong polarization electric field in the AlGaIn/

Received: July 30, 2019

Accepted: October 21, 2019

Published: October 21, 2019

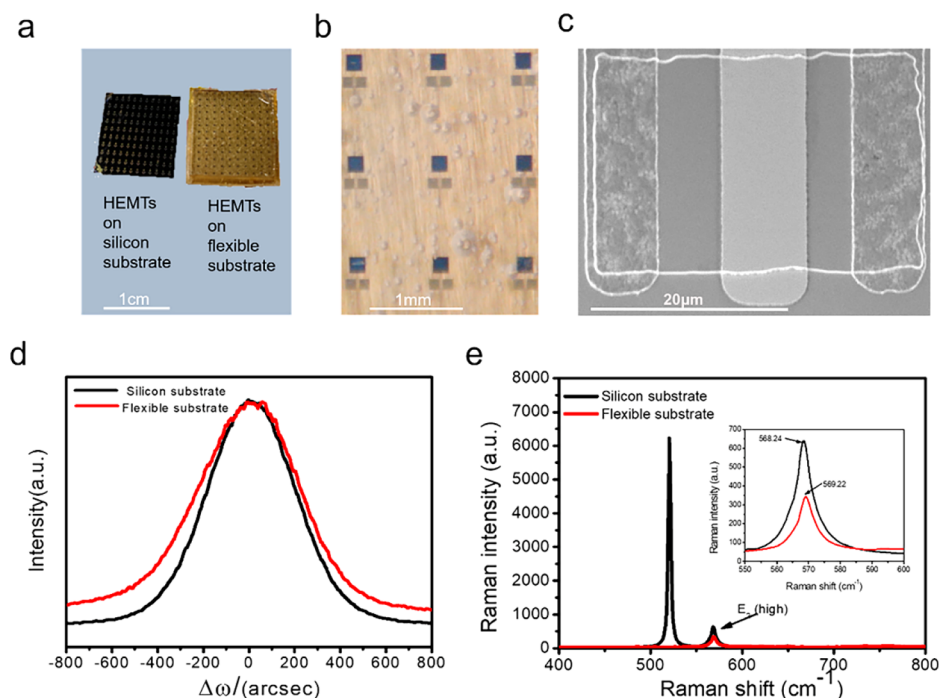


Figure 1. (a) Optical pictures of HEMTs before and after substrate transfer. (b) A microphotograph of the 3×3 HEMTs arrays. (c) SEM image of a single flexible HEMT. (d) Rocking curves of GaN (002) plane before and after transfer. (e) Raman spectroscopy of AlGaIn/GaN HEMTs before and after substrate transfer.

GaN heterojunction and a high-density two-dimensional electron gas (2DEG) at the heterojunction interface.^{13–15} The external stress is proved to significantly alter the energy band structure in the AlGaIn/AlN/GaN heterojunction interface, which can effectively modulate electrical characteristics.¹⁴ Based on this mechanism, the stress modulated HEMTs were successfully fabricated by thinning Si substrate.¹⁶ These devices build a real-time, sensitive, and seamless interaction between the external weak mechanical stimuli and high-power output, thus exhibiting great potential in human–machine interface, smart sensing, mechanical energy harvesting, and robotics and so on. However, although substrate thinning technology improves the mechanical flexibility, it has a limited modulation range. Enduring higher mechanical deformation is a significant direction for flexible piezotronic devices,¹⁷ and flexible HEMTs can achieve it.

In this paper, we proposed a low damage and wafer-scale substrate transfer technology to fabricate flexible AlGaIn/AlN/GaN HEMTs arrays. With this technology, 10×12 AlGaIn/AlN/GaN HEMTs arrays (1.3×1.3 cm² wafer area) were perfectly transferred from the silicon substrate to a flexible copper substrate, and the electrical properties had a few losses and reached an excellent level in flexible HEMTs devices. More importantly, the flexible HEMTs greatly enhance the toleration of mechanical deformation to achieve a much more effective stress modulation on the output power density. These piezotronic effect modulated flexible HEMTs may have broad application prospects in the fields of human–machine interface, active sensors, and intelligent microinductor system, etc.

RESULTS AND DISCUSSION

Figure 1a shows the optical pictures of HEMTs before and after transfer. A large-scale HEMTs arrays (10×12 HEMTs and 1.3×1.3 cm² wafer area) were fabricated on the silicon

substrate. The optical picture (the left one) clearly shows well-aligned arrays and a black silicon substrate. The optical picture of flexible HEMTs (the right one) proved that these large-scale and well-aligned HEMTs arrays were perfectly transferred to the yellow copper flexible substrate. Figure 1b is a microphotograph of the 3×3 HEMTs arrays, from which we can find that the arrays and the devices are intact. The SEM image of single flexible HEMTs is shown in the Figure 1c, and there is not any damage on source/drain/gate electrodes. These morphology characterizations show our transfer technology can achieve wafer-scale and well-aligned HEMTs arrays with unbroken device structures.

The crystal quality is a key material property to affect device performances. The high-resolution X-ray diffraction (HRXRD) measurements were performed to evaluate the crystal qualities of the AlGaIn/GaN heterojunction before and after transfer. The Rocking curves of GaN (002) plane before and after transfer are shown in Figure 1d. The full width at half-maximum (fwhm) of GaN (002) plane on silicon substrate was 425 arcsec, and after transferred to the copper flexible substrate, the fwhm slightly increases to 509 arcsec. The (002) diffraction is connected with the screw dislocation, and the fwhm value of the Rocking curve is related to the density of screw dislocation, according to eq 1:¹⁸

$$D_{\text{screw}} = \frac{\beta^2}{4.36b^2} \quad (1)$$

where D_{screw} is the screw dislocation density, β is the fwhm value of the Rocking curve, and b is the Burger vector. We can deduce the dislocation density before and after transfer to be 3.62×10^8 cm⁻² and 5.12×10^8 cm⁻², respectively. There is a slight increase in the dislocation density in the layer. In addition, the carrier mobility is an important parameter for AlGaIn/GaN materials. We measured the carrier mobility (μ)

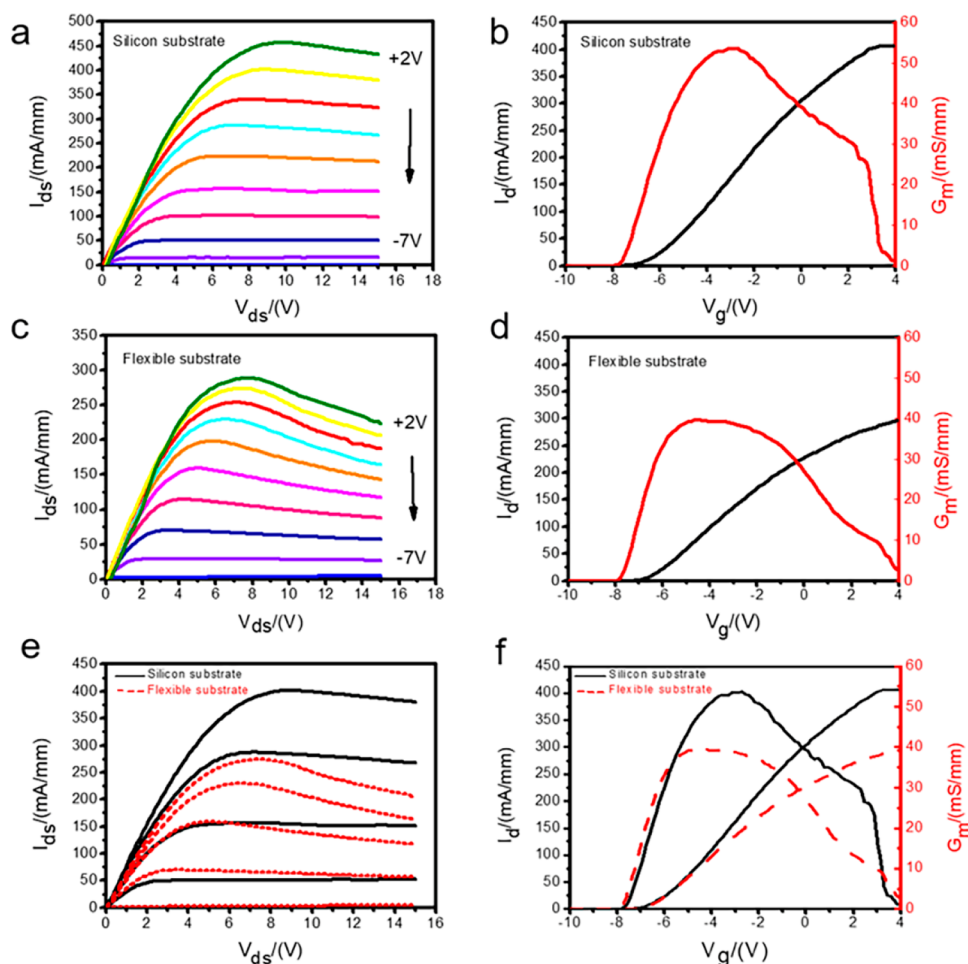


Figure 2. Electrical properties of HEMT devices. (a) Output curves (with gate bias from -7 V to $+2$ V from bottom to top with step by 1 V) and (b) transfer characteristics of HEMTs on silicon substrate. (c) Output curves (with gate bias from -7 V to $+2$ V from bottom to top with step by 1 V) and (d) transfer characteristics of flexible HEMTs. (e, f) Graphs of electrical properties comparisons of HEMTs devices on different substrates.

before and after substrate transfer by Hall test, as shown in Table S1. According to Table S1, we can find that the mobility is 1626 $\text{cm}^2/\text{V}\cdot\text{s}$ and 1591 $\text{cm}^2/\text{V}\cdot\text{s}$ on the silicon substrate and the flexible substrate, respectively. We can conclude that the mobility decreases little after substrate transfer with a drop of 2% . These experiments prove that our transfer technology causes few damages on the crystal and material properties.

Due to the large lattice mismatch and thermal mismatch between the GaN film and the Si substrate, there is often residual stress in the epitaxial layer.¹⁹ In general, changes in the material type and the thickness of the substrate would have an effect on the internal residual stress. The micro-Raman spectroscopy is used to measure the change of the internal lattice state, thereby obtaining the change of the internal residual stress.²⁰ Since the Raman E_2 -high phonon mode peak of GaN is sensitive to the stress state of GaN, the internal residual stress change of the GaN layer can be estimated by observing the relative movement of E_2 -high.²¹ The Raman spectrum in Figure 1e shows that the E_2 -high peak position of GaN after the substrate transfer is blue-shifted. The peak value after transfer (569.22 cm^{-1}) is higher than the previous peak value (568.84 cm^{-1}). The relationship between the residual stress and the material peak shift is shown in eq 2:

$$\sigma_a = -\frac{\Delta\omega}{\kappa_{\text{Ra},a}} \quad (2)$$

where σ_a is the residual stress, $\Delta\omega$ is the offset value of peak position, $\kappa_{\text{Ra},a}$ is the Raman correction factor. According to calculations, the GaN epitaxial layer is subjected to a decreased tensile stress of 245 MPa compared with that on the Si substrate. Due to the larger lattice constant of silicon substrates, the GaN wafer coherent grown on silicon substrate is commonly under a very strong tensile stress. After lifting-off and transferring to a flexible copper substrate, the tensile stress will be partly released, a 245 MPa decrease in our experiments.

The DC output current–voltage ($I_{\text{ds}}-V_{\text{ds}}$) and transfer properties were measured by a Keysight B1500 semiconductor parameter analyzer. The $I_{\text{ds}}-V_{\text{ds}}$ characteristic curves of AlGaIn/GaN HEMTs on silicon substrate were shown in Figure 2a (with V_{gs} ranging from $+2$ V to -7 V with step by 1 V from top to bottom). When the gate-source voltage (V_{gs}) of the device is less than its threshold voltage (V_{th}), the negative gate bias completely depletes the electrons at the interface under the gate heterojunction, causing the conductive channel to be disconnected, and the device is in an off state. We can conclude from Figure 2a that when $V_{\text{gs}} = -7$ V (less than V_{th}), the source leakage current is very small, indicating the device has good low leakage characteristics in this case. When V_{gs} is

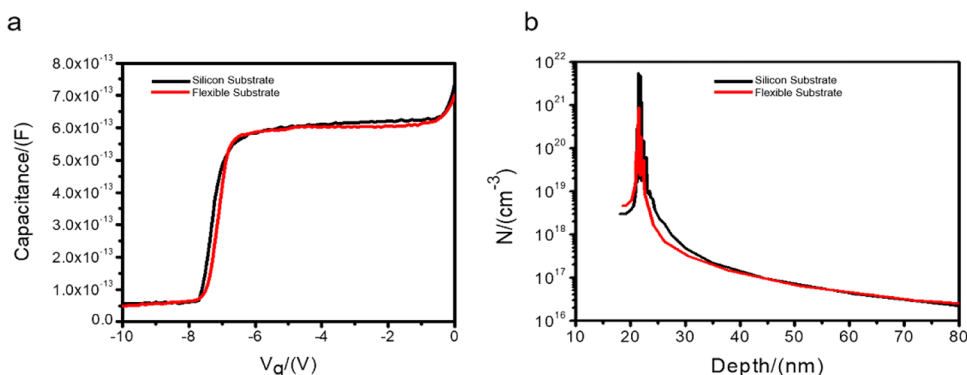


Figure 3. Capacitance–voltage (C – V) curves of AlGaIn/GaN HEMTs on silicon substrate and flexible substrate (a) C – V profiles. (b) Carrier concentration as a function of depletion depth.

greater than V_{th} , the I_{ds} – V_{ds} characteristic curves of AlGaIn/GaN HEMTs can be divided into a linear region and saturated region. When the drain-source voltage (V_{ds}) is small, the device works in the linear region, and the increase in output current is consistent with the change in drain-source voltage. When the V_{ds} is large, the channel electron drift speed becomes saturated, and the drain-source current also saturates, so the device operates in saturated region. In addition, under different biases, the maximum saturated drain-source current density ($I_{d,max}$) increases as V_{gs} increases. According to Figure 2a, we can find that the HEMTs device achieves $I_{d,max} = 457$ mA/mm at a positive gate voltage of +2 V. The transfer characteristic curves of AlGaIn/GaN HEMTs on silicon substrate are shown in Figure 2b (with $V_{ds} = 10$ V). It can be found from the Figure 2b that the maximum transconductance ($g_{m,max}$) of the HEMTs on Si substrate is 53 mS/mm.

Figure 2c,d shows the I_{ds} – V_{ds} and transfer characteristic curves of flexible AlGaIn/GaN HEMTs, respectively. I – V plots also have the typical electrical characteristics of HEMTs devices. In the off state (when $V_{gs} = -7$ V), the source leakage current of the flexible HEMT is also low, indicating that the surface defect state is not increased after the substrate transfer and the off-state electrical properties of the flexible HEMTs are not changed. Besides, the maximum saturated drain current density ($I_{d,max}$) of the flexible HEMTs is approximately 290 mA/mm at $V_{gs} = +2$ V and the $g_{m,max}$ is 40 mS/mm, which demonstrates that the flexible HEMTs also have excellent electrical performances. Figure 2e,f shows the electrical property comparisons of HEMTs devices on different substrates. From Figure 2e,f, we find that the maximum saturated drain current and the maximum transconductance of AlGaIn/GaN HEMTs on the flexible substrate are lower than that on Si substrates. Besides, another notable feature in Figure 2e is that the I_{ds} – V_{ds} characteristic curves of flexible HEMTs have significant current collapse in saturated regions. In this paper, although the electrical properties of the HEMTs devices decrease after substrate transfer, the devices still have excellent performances among the previous studies, as shown in Table S2. According to Table S2, our flexible HEMTs devices have excellent performances compared to the previous studies. Besides, the ratio of electrical performances degradation before and after transfer is relatively smallest among the previous studies.

The performance loss is an unavoidable problem in the process of flexibility. There are many reasons for the current decrease of flexible devices, such as stress state change,²² trap effects,²³ and self-heating effects,^{24,25} etc. From the Raman

spectrum in Figure 1e, it can be concluded that after lifting-off and transferring to a flexible copper substrate, the tensile stress will be partly released, a 245 MPa decrease in our research. That is to say the stress state changes in the GaN layer after substrate transfer, which may have an effect on the electrical properties. The 2DEG density is proper for the piezoelectric polarization charge, and the reduced 2DEG density will decrease the saturated current. In order to verify whether the 2DEG density changed after substrate transfer, we performed capacitance–voltage (C – V) measurements in this research. The C – V measurements (at 1 MHz) curves of HEMTs devices before and after substrate transfer are plotted in Figure 3a. We can calculate the sheet density of 2DEG based on the capacitance–voltage (C – V). It can be seen from the C – V curves that the sheet density of the 2DEG on the AlGaIn/AlN/GaN heterojunctions can be expressed by eq 3a:

$$n_s = \frac{1}{qA} \int C dV \quad (3a)$$

where n_s is the sheet density of the 2DEG, q is the elementary charge, A is the contact area, C is the capacitance, and V is the voltage. By integrating the C – V curves, we can calculate that the sheet densities are 1.02×10^{13} cm⁻² and 0.97×10^{13} cm⁻² before and after transfer, respectively. There is a 5% drop in sheet density of 2DEG, and it shows that the change in residual stress state of the GaN layer does have an effect on the density of 2DEG after transfer. From the C – V measurement, the carrier distribution profiles can be calculated according to the following equations:

$$N = \frac{C^3}{\epsilon \epsilon_0 \epsilon A^2} \frac{dV}{dC} \quad (3b)$$

$$Z = \frac{\epsilon_0 \epsilon A}{C} \quad (3c)$$

where N is the carrier density, Z is the thickness of carrier, and ϵ is the relative dielectric constant of the semiconductor material. The carrier distribution profiles are shown in Figure 3b. It can be seen from Figure 3b that the confinement of 2DEG remains unchanged, since the 2DEG is located within 2–3 nm in the heterojunctions barrier layer. Substrate transferred process inevitably induces defects to scatter carriers, which decreases 2DEG concentration and finally degrades electrical characteristics of HEMTs devices.²⁶ Therefore, the trap effects may be a cause of the current drop. The self-heating effect causes the device temperature to rise,

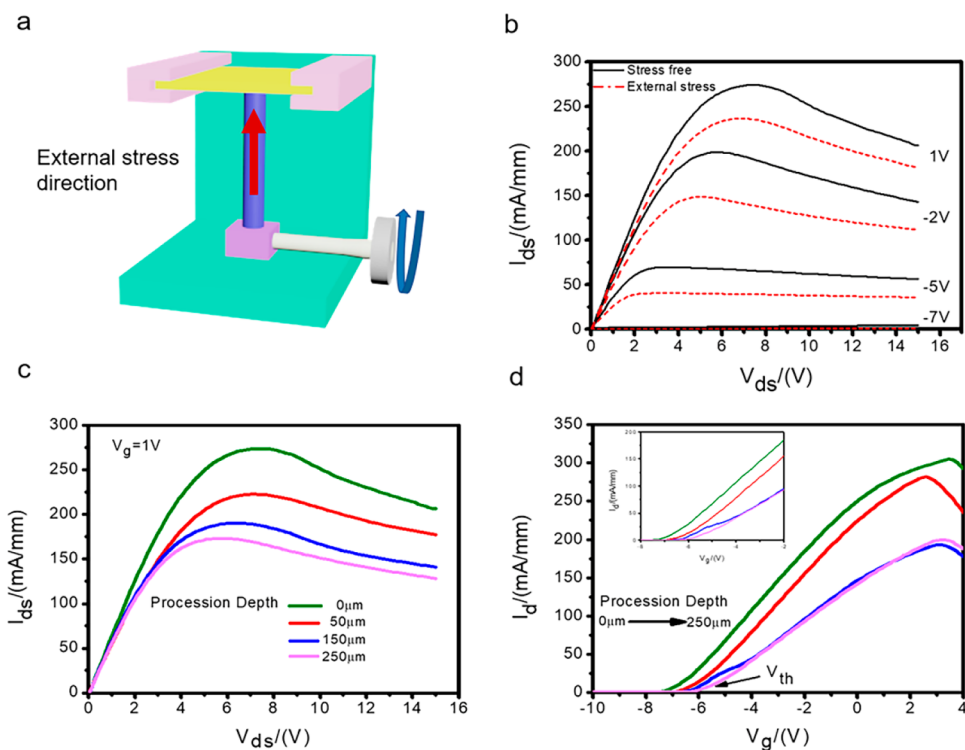


Figure 4. (a) Devices for applying external stress. (b) I_{ds} – V_{ds} curves of HEMTs devices with applied external stress. (c) I_{ds} – V_{ds} curves of HEMTs devices under different procession distances (indicating the external stress increases from top to bottom). (d) Transfer characteristics of HEMTs devices under different procession distances.

enhancing phonon scattering, thereby leading to a decrease of carrier mobility in the potential well, which can have an impact on the static I – V characteristics of the device. Among common heat dissipation materials, the copper has a very good thermal conductivity. This is another reason why we choose it as the substrate of the flexible HEMTs. However, to adhere the flexible HEMTs to the copper substrate, we took the epoxy adhesive, which had poor thermal conductivity compared to the silicon substrate, thus the devices had not good heat dissipation. Therefore, the electrical characteristics of the device deteriorate on the flexible substrate, causing a drop in saturated current and a collapse in current. We can further improve the performances of HEMTs by optimizing the thickness of epoxy adhesive or choosing higher conductivity binders.²⁷

The AlGaIn/GaN heterojunction has a strong spontaneous polarization (P_{sp}) and piezoelectric polarization (P_{pe}), due to the noncentral symmetry and the lattice mismatch.²⁸ Under external stress, the lattices of AlGaIn and GaN will be deformed, thereby inducing polarization charges and generating piezotronic effect. The piezotronic effect affects the distribution of free carriers and can significantly modulate the band structure of the AlGaIn/GaN heterojunction. The piezotronic effect provides a different freedom to optimize device performances and introduces an opportunity to sensing or feedback external mechanical stimuli. The piezotronic effect measurements are performed by a special instrument, as shown in Figure 4a. We can adjust the knob to control the procession distance, which can characterize the different external stress applied to the sample. Compared to the rigid silicon substrate, the thin copper substrate exhibits a very good flexibility. Even with large bending, no cracks were observed on the AlGaIn/AlN/GaN wafers and no electrode shedding occurred on any

source-gate-drain electrodes in 10×12 HEMTs arrays. The I_{ds} – V_{ds} curves of the HEMTs under stress free and under external stress are plotted in Figure 4b. It is obvious that the I_{ds} of the device decreases when external stress is applied. In addition, the current variations of the HEMTs device under different external stress are shown in Figure 4c at $V_g = 1$ V (procession distance increasing from top to bottom). It can be found from Figure 4c that as the procession distance increases (indicating the external stress increasing), the I_{ds} gradually reduces, which is closely related to the 2DEG at AlGaIn/GaN heterojunction modulated by the piezotronic effect. The piezotronic effect modulation mechanism has been discussed before.^{29,30} The external stress causes negative piezoelectric charge accumulating at the heterojunction interface, thus the energy band on the GaN side is raised, resulting the triangular potential well at the heterojunction interface to become shallow. The concentration of 2DEG decreases, thereby reducing the saturated current of the HEMTs device.¹⁴ Figure 4d is the corresponding transfer characteristic curves. It can be concluded that as the stress increases, the threshold voltage (V_{th}) shifts positively. The expression of the threshold voltage is as follows:^{31,32}

$$V_{th} = \frac{\Phi_b}{e} - \frac{\Delta E_c}{e} - \frac{d\sigma_{pol}}{\epsilon\epsilon_0} \quad (4)$$

where V_{th} is the threshold voltage of AlGaIn/GaN HEMTs, Φ_b is the Schottky barrier height, ΔE_c is the AlGaIn/GaN heterojunction interface conduction band offset, and σ_{pol} is the total polarization charge density at the heterojunction interface. The σ_{pol} can characterize 2DEG density at the heterojunction. According to eq 4, we can conclude that the 2DEG density has a positive correlation with the absolute value

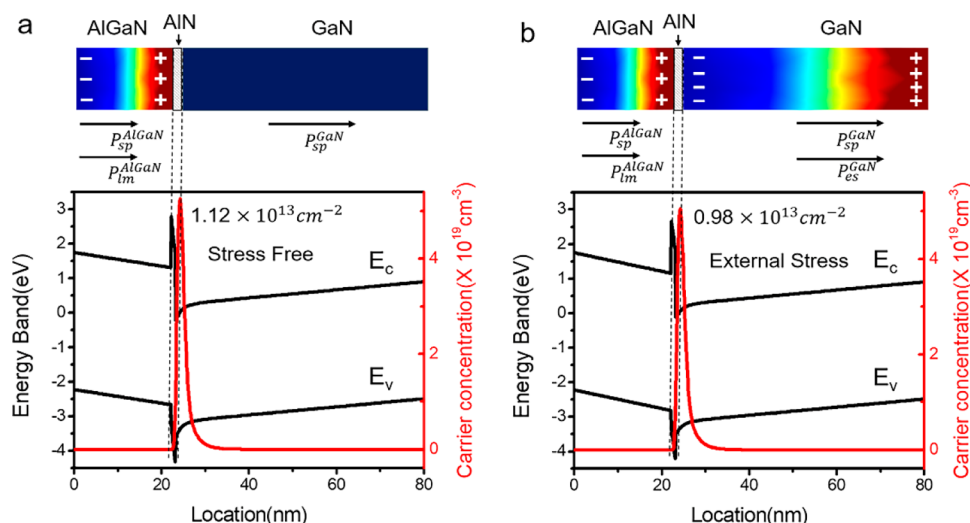


Figure 5. Band diagrams at the interface of AlGaIn/GaN heterojunction. (a) Under stress free. (b) Under external stress.

of the threshold voltage. Therefore, the threshold voltage moves to a positive value, indicating that the 2DEG density at the heterojunction has a decreasing trend, which is consistent with the change in electrical performances of HEMTs. These analyses illustrate that the piezotronic effect can effectively modulate the electrical properties of flexible HEMTs.

In order to further understand the relationship between the change of electrical properties and the piezotronic effect, we obtained the energy band diagrams of the AlGaIn/GaN heterojunction by the self-consistent calculation of Schrödinger equation and Poisson equation, as shown in Figure 5. The physical parameters of wurtzite structure AlN and GaN are shown in Table S3. Under stress free condition, there are spontaneous polarizations P_{SP}^{AlGaIn} , P_{SP}^{GaN} due to noncoincidence of positive and negative charge centers in AlGaIn and GaN and piezoelectric polarization P_{lm}^{AlGaIn} due to lattice mismatch in AlGaIn layer. Under the electric field caused by P_{SP}^{AlGaIn} , P_{SP}^{GaN} , and P_{lm}^{AlGaIn} , the electrons are trapped in a triangular potential well in the AlGaIn/GaN heterojunction interface to form 2DEG, as shown in Figure 5a. For the mesa-isolated AlGaIn/GaN heterojunction, the size of the AlGaIn isolation island is much smaller than the size of the entire epitaxial wafer, so it can be considered that the external stress applied to the back of the device is hardly transmitted to the AlGaIn layer. Therefore, the external stress does not change the stress state of the AlGaIn layer, but only changes the stress state of the GaN layer.³³ The application of external stress changes the AlGaIn/GaN heterojunction band is shown in Figure 5b. The external stress generates piezoelectric polarization in the GaN layer, thus the negative piezoelectric charge accumulates at the heterojunction interface, raising the energy band on the GaN side and making the triangular potential well at the heterojunction interface to shallow. The shallower potential well causes the ability of binding carriers to be weak, and the 2DEG concentration reduces, so the saturated current of the HEMTs device decreases. As the external stress increases, this modulation is also strengthened. It further illustrates that the piezotronic effect can modulate the flexible HEMTs.

CONCLUSIONS

In conclusion, we have successfully fabricated flexible AlGaIn/GaN HEMTs arrays through a low-damage and wafer-scale

substrate transfer technology from a rigid Si substrate. The flexible HEMTs have excellent electrical performances with the maximum saturated drain current density ($I_{d,max}$) achieving approximate 290 mA/mm at $V_{gs} = +2$ V and the maximum transconductance ($g_{m,max}$) reaching to 40 mS/mm. The performance loss is an unavoidable problem in the process of flexibility. There are many reasons that are responsible for the decline in the electrical performances of HEMTs devices, such as stress state change, trap effects, and self-heating effects, etc. The flexible HEMTs can endure the larger mechanical distortion, and the piezotronic effect provides a different freedom to optimize device performances. Based on the piezotronic effect, we introduced an external stress to modulate the electrical performances of flexible HEMTs. The experimental results show that the piezotronic effect can significantly modulate the electrical properties of HEMTs devices. The piezotronic effect introduces an opportunity to sense or feedback external mechanical stimuli. The piezotronic effect modulated flexible HEMTs exhibit great potential in human-machine interfaces, intelligent microinductor systems, smart sensing, and so on.

METHODS

Transistors Fabrication on Silicon Substrate. The AlGaIn/GaN heterojunction was grown on Si substrate (111) by metal organic chemical vapor deposition (MOCVD). The epitaxial wafer consists of a 20 nm AlGaIn barrier layer with an Al content of 30%, a 1 nm AlN interlayer, 300 nm unintentionally doped GaN channel layer, and a 3.5 μ m-thick carbon-doped GaN buffer layer. Before the device was fabricated, the surface of the epitaxial wafer was cleaned with acetone and ethanol for several times. Then dry etching was performed by inductively coupled plasma (ICP) to form isolation regions, followed by photolithography to form electrode patterns. The metal electrodes were deposited by electron beam evaporation to fabricate corresponding electrodes. Four layers of metal Ti/Al/Ni/Au (20/120/45/55 nm) were deposited as the source and drain electrodes and then rapid thermal annealed in N_2 environment at 850 $^{\circ}C$ for 30 s to form an ohmic contact. The gate electrode needs Schottky contact, which can be realized by depositing Ni/Au (80/50 nm) with the electron beam evaporation.³⁴ Keysight B1500 semiconductor parameter analyzer is used to measure the device DC characteristics at room temperature.

Fabrication of Flexible HEMTs. We proposed a method for wafer-scale transfer HEMT arrays from a rigid Si substrate to a flexible substrate. The main steps of substrate transfer technology are shown

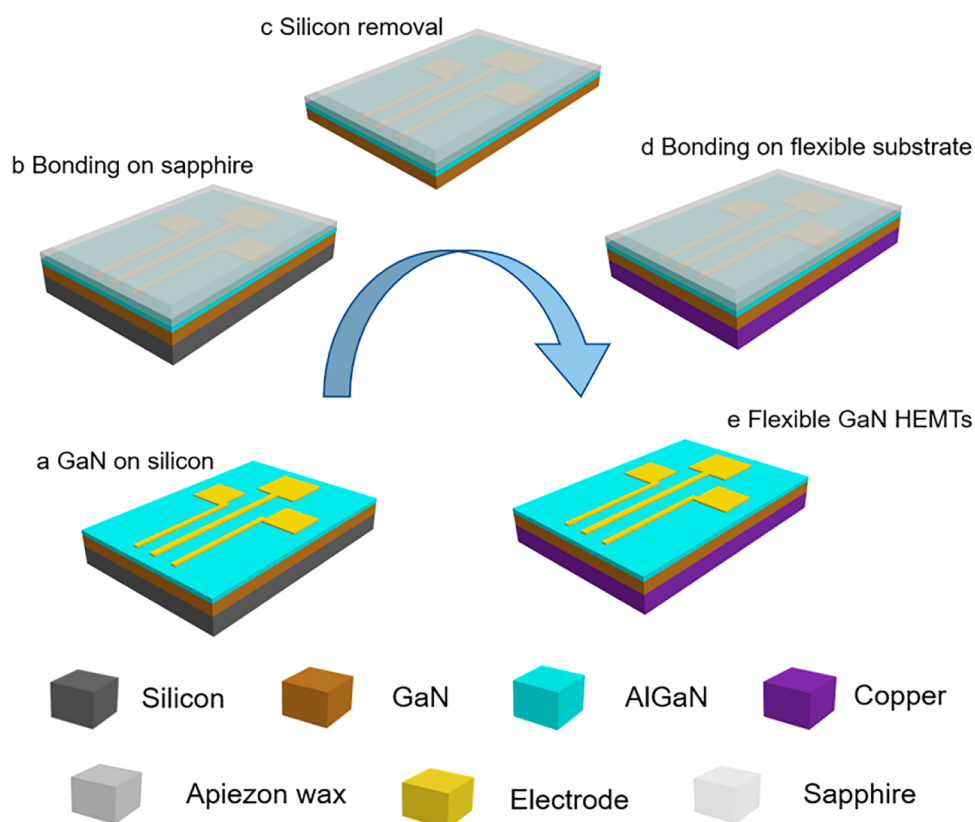


Figure 6. Main steps of substrate transfer technology.

in Figure 6. A thick layer of resist was coated on the surface of the device in the first step in transfer process, where the resist was Apiezon wax. The resist layer protected the devices and acted as adhesive layer to bond the front side of the device to a temporary carrier. Next chemical etching was used to remove silicon substrate. This wet etching was based on $\text{HNO}_3/\text{HF}/\text{CH}_3\text{COOH}$ solution, and the etching rate was about $5 \mu\text{m}/\text{min}$. After the Si substrate was completely removed, the back side was adhered to a flexible copper substrate with epoxy adhesive. Then the front resist layer (Apiezon wax) was removed with toluene or chloroform and separated from the temporary carrier.

ASSOCIATED CONTENT

Supporting Information

The Supporting Information is available free of charge on the ACS Publications website at DOI: 10.1021/acsnano.9b05999.

The parameters on devices before and after transfer; the performances of our research among the previous studies; the physical parameters of wurtzite structure AlN and GaN (PDF)

AUTHOR INFORMATION

Corresponding Authors

*E-mail: huweigu@binn.cas.cn.

*E-mail: zlwang@gatech.edu.

ORCID

Weigu Hu: 0000-0002-8614-0359

Zhong Lin Wang: 0000-0002-5530-0380

Author Contributions

#These authors contributed equally to this work.

Notes

The authors declare no competing financial interest.

ACKNOWLEDGMENTS

The authors thank for the support from National Natural Science Foundation of China (grant nos. 51432005, 61574018, and 61704008) and National Key Research and Development Program of China (2016YFA0202703).

REFERENCES

- (1) Nathan, A.; Ahnood, A.; Cole, M. T.; Lee, S.; Suzuki, Y.; Hiralal, P.; Bonaccorso, F.; Hasan, T.; Garcia-Gancedo, L.; Dyadyusha, A.; Haque, S.; Andrew, P.; Hofmann, S.; Moultrie, J.; et al. Flexible Electronics: The Next Ubiquitous Platform. *Proc. IEEE* **2012**, *100*, 1486–1517.
- (2) Lee, K. J.; Meitl, M. A.; Ahn, J. H.; Rogers, J. A.; Nuzzo, R. G.; Kumar, V.; Adesida, I. Bendable GaN High Electron Mobility Transistors on Plastic Substrates. *J. Appl. Phys.* **2006**, *100*, 124507.
- (3) Jiang, C.; Liu, T.; Du, C.; Huang, X.; Liu, M.; Zhao, Z.; Li, L.; Pu, X.; Zhai, J.; Hu, W.; Wang, Z. L. Piezotronic Effect Tuned AlGaIn/GaN High Electron Mobility Transistor. *Nanotechnology* **2017**, *28*, 114894.
- (4) Jiang, J.; Wang, Q.; Wang, B.; Dong, J.; Li, Z.; Li, X.; Zi, Y.; Li, S.; Wang, X. F. Direct Lift-Off and the Piezo-Phototronic Study of InGaIn/GaN Heterostructure Membrane. *Nano Energy* **2019**, *59*, 545–552.
- (5) Lesecq, M.; Hoel, V.; Lecavelier Des Etangs-Levallois, A.; Pichonat, E.; Douvry, Y.; De Jaeger, J. C. High Performance of AlGaIn/GaN HEMTs Reported on Adhesive Flexible Tape. *IEEE Electron Device Lett.* **2011**, *32*, 143–145.
- (6) Kobayashi, Y.; Kumakura, K.; Akasaka, T.; Makimoto, T. Layered Boron Nitride As a Release Layer for Mechanical Transfer of GaN-Based Devices. *Nature* **2012**, *484*, 223–227.
- (7) Mhedhbi, S.; Lesecq, M.; Altuntas, P.; Defrance, N.; Cordier, Y.; Damilano, B.; Tabares Jimenez, G.; Ebongue, A.; Hoel, V. Recent Improvements of Flexible GaN-Based HEMT Technology. *Phys. Status Solidi A* **2017**, *214*, 1600484.

- (8) Peng, Y.; Que, M.; Lee, H.; Bao, R.; Wang, X.; Lu, J.; Yuan, Z.; Li, X.; Tao, J.; Sun, J.; Zhai, J.; Lee, K.; Pan, C. F. Achieving High-Resolution Pressure Mapping via Flexible GaN/ZnO Nanowire LEDs Array by Piezo-Phototronic Effect. *Nano Energy* **2019**, *58*, 633–640.
- (9) Wang, X.; Zhou, J.; Song, J.; Liu, J.; Xu, N.; Wang, Z. L. Piezoelectric Field Effect Transistor and Nanoforce Sensor Based on a Single ZnO Nanowire. *Nano Lett.* **2006**, *6*, 2768–2772.
- (10) Wang, Z. L. Nanopiezotronics. *Adv. Mater.* **2007**, *19*, 889–892.
- (11) Wang, Z. L. Progress in Piezotronics and Piezo-Phototronics. *Adv. Mater.* **2012**, *24*, 4632–4646.
- (12) Hu, Y.; Zhang, Y.; Chang, Y.; Snyder, R. L.; Wang, Z. L. Optimizing the Power Output of a ZnO Photocell by Piezopotential. *ACS Nano* **2010**, *4*, 4220–4224.
- (13) Huang, X.; Du, C.; Zhou, Y.; Jiang, C.; Pu, X.; Liu, W.; Hu, W.; Chen, H.; Wang, Z. L. Piezo-Phototronic Effect in a Quantum Well Structure. *ACS Nano* **2016**, *10*, 5145–5152.
- (14) Wang, X.; Yu, R.; Jiang, C.; Hu, W.; Wu, W.; Ding, Y.; Peng, W.; Li, S.; Wang, Z. L. Piezotronic Effect Modulated Heterojunction Electron Gas in AlGaIn/GaN Heterostructure Microwire. *Adv. Mater.* **2016**, *28*, 7234–7242.
- (15) Zhao, Z.; Pu, X.; Han, C.; Du, C.; Li, L.; Jiang, C.; Hu, W.; Wang, Z. L. Piezotronic Effect in Polarity Controlled GaN Nanowires. *ACS Nano* **2015**, *9*, 8578–8583.
- (16) Liu, T.; Jiang, C.; Huang, X.; Du, C.; Zhao, Z.; Jing, L.; Li, X.; Han, S.; Sun, J.; Pu, X.; Zhai, J.; Hu, W. G. Electrical Transportation and Piezotronic-Effect Modulation in AlGaIn/GaN MOS HEMTs and Unpassivated HEMTs. *Nano Energy* **2017**, *39*, 53–59.
- (17) Hu, G.; Guo, W.; Yu, R.; Yang, X.; Zhou, R.; Pan, C.; Wang, Z. L. Enhanced Performances of Flexible ZnO/Perovskite Solar Cells by Piezo-Phototronic Effect. *Nano Energy* **2016**, *23*, 27–33.
- (18) Gay, P.; Hirsch, P. B.; Kelly, A. The Estimation of Dislocation Densities in Metals from X-Ray Data. *Acta Metall.* **1953**, *1*, 315–319.
- (19) Liu, K.; Zhu, H.; Feng, S.; Shi, L.; Zhang, Y.; Guo, C. The Effect of External Stress on the Electrical Characteristics of AlGaIn/GaN HEMTs. *Microelectron. Reliab.* **2015**, *55*, 886–889.
- (20) Briggs, R. J.; Ramdas, A. K. Piezospectroscopic Study of the Raman Spectrum of Cadmium Sulfide. *Phys. Rev. B* **1976**, *13*, 5518–5529.
- (21) Kisielowski, C.; Kruger, J.; Ruvimov, S.; Suski, T.; Ager, J. W.; Jones, E.; Liliental-Weber, Z.; Rubin, M.; Weber, E. R.; Bremser, M. D.; Davis, R. F. Strain-Related Phenomena in GaN Thin Films. *Phys. Rev. B: Condens. Matter Mater. Phys.* **1996**, *54*, 17745.
- (22) Azize, M.; Palacios, T. Effect of Substrate-Induced Strain in the Transport Properties of AlGaIn/GaN Heterostructures. *J. Appl. Phys.* **2010**, *108*, 023707.
- (23) Faqir, M.; Verzellesi, G.; Meneghesso, G.; Zanoni, E.; Fantini, F. Investigation of High-Electric-Field Degradation Effects in AlGaIn/GaN HEMTs. *IEEE Trans. Electron Devices* **2008**, *55*, 1592–1602.
- (24) Nazari, M.; Hancock, B. L.; Piner, E. L.; Holtz, M. W. Self-Heating Profile in an AlGaIn/GaN Heterojunction Field-Effect Transistor Studied by Ultraviolet and Visible Micro-Raman Spectroscopy. *IEEE Trans. Electron Devices* **2015**, *62*, 1467–1472.
- (25) Mhedhbi, S.; Lesecq, M.; Altuntas, P.; Defrance, N.; Okada, E.; Cordier, Y.; Damilano, B.; Tabares-Jimenez, G.; Ebongue, A.; Hoel, V. First Power Performance Demonstration of Flexible AlGaIn/GaN High Electron Mobility Transistor. *IEEE Electron Device Lett.* **2016**, *37*, 553–555.
- (26) Sahoo, D. K.; Lal, R. K.; Hyungtak, K.; Tilak, V.; Eastman, L. F. High-Field Effects in Silicon Nitride Passivated GaN MODFETs. *IEEE Trans. Electron Devices* **2003**, *50*, 1163–1170.
- (27) Defrance, N.; Lecourt, F.; Douvry, Y.; Lesecq, M.; Hoel, V.; Lecavelier Des Etangs-Levallois, A.; Cordier, Y.; Ebongue, A.; De Jaeger, J. C. Fabrication, Characterization, and Physical Analysis of AlGaIn/GaN HEMTs on Flexible Substrates. *IEEE Trans. Electron Devices* **2013**, *60*, 1054–1059.
- (28) Wang, Z. L.; Song, J. Piezoelectric Nanogenerators Based on Zinc Oxide Nanowire Arrays. *Science* **2006**, *312*, 242–246.
- (29) Jiang, C.; Jing, L.; Huang, X.; Liu, M.; Du, C.; Liu, T.; Pu, X.; Hu, W.; Wang, Z. L. Enhanced Solar Cell Conversion Efficiency of InGaIn/GaN Multiple Quantum Wells by Piezo-Phototronic Effect. *ACS Nano* **2017**, *11*, 9405–9412.
- (30) Jiang, C.; Chen, Y.; Sun, J.; Jing, L.; Liu, M.; Liu, T.; Pan, Y.; Pu, X.; Ma, B.; Hu, W.; Wang, Z. L. Enhanced Photocurrent in InGaIn/GaN MQWs Solar Cells by Coupling Plasmonic with Piezo-Phototronic Effect. *Nano Energy* **2019**, *57*, 300–306.
- (31) Delagebeaudeuf, D.; Linh, N. T. Metal-(n) AlGaAs-GaAs Two-Dimensional Electron Gas FET. *IEEE Trans. Electron Devices* **1982**, *29*, 955–960.
- (32) Ridley, B. K. Analytical Models for Polarization-Induced Carriers. *Semicond. Sci. Technol.* **2004**, *19*, 446–450.
- (33) Kang, B. S.; Kim, S.; Kim, J.; Ren, F.; Baik, K.; Pearton, S. J.; Gila, B. P.; Abernathy, C. R.; Pan, C.; Chen, G.; Chyi, J. I.; Chandrasekaran, V.; Sheplak, M.; Nishida, T.; Chu, S. N. G. Effect of External Strain on the Conductivity of AlGaIn/GaN High-Electron-Mobility Transistors. *Appl. Phys. Lett.* **2003**, *83*, 4845–4847.
- (34) Gong, R.; Wang, J.; Liu, S.; Dong, Z.; Yu, M.; Wen, C.; Cai, Y.; Zhang, B. Analysis of Surface Roughness in Ti/Al/Ni/Au Ohmic Contact to AlGaIn/GaN High Electron Mobility Transistors. *Appl. Phys. Lett.* **2010**, *97*, 062115.